Soft Matter

Accepted Manuscript

ROYAL SOCIETY OF CHEMISTRY

www.rsc.org/softmatter

Soft Matter

RSCPublishing

COMMUNICATION

Cite this: DOI: 10.1039/x0xx00000x

Bioadhesive giant vesicles for monitoring hydroperoxidation in lipid membranes

Received ooth January 2012,
Accepted ooth January 2012

DOI: 10.1039/x0xx00000x

www.rsc.org/

P. H. B. Aoki,[a,b,c] A. P. Schroder,[a] C. J. L. Constantino[b] and C. M. Marques[a]

Soft Matter

RSCPublishing

COMMUNICATION

Osmotic stresses, protein insertion or lipid oxidation lead to area increase of self-assembled lipid membranes. However, methods to measure membrane expansion are scarce. Challenged by recent progress on the control of phospholipid hydroperoxidation, we introduce a method to quantitatively evaluate membrane area increase based on the bio-adhesion of Giant Unilamellar Vesicles.

Lipid photo-oxidation is a natural outcome of life under oxygen and essential for Photodynamic Therapy of cancer tissues.[1-2] Hydroperoxidation, a prominent pathway for lipid oxidation, results in the insertion of the organic hydroperoxide group OOH at the unsaturated bond site.[3-5] At the molecular level, the increased hydrophilicity of the lipid chains carrying the OOH groups changes the statistical distribution of chain conformations and leads noticeably to the increase of the area per lipid. Degree of membrane oxidation, and the associated changes in membrane properties such as membrane shape, elasticity or permeability[6-8] can thus be monitored by a measure of membrane area increase.

Previous methods to monitor membrane area changes following oxidation relied on the application of micropipette suction techniques or external electric fields to Giant Unilamellar Vesicles (GUVs).[7-8] While micropipette suction recently provided the first values for oxidized lipid area expansions, its implementation is not straightforward. In particular, pipettes have to be pulled and forged, coupled to a hydrostatic device before being monitored in the microscope objective vicinity through a high precision, i.e. micrometer range, XYZ manipulation device. Measuring membrane deformation by electric fields is more straightforward and contactless, requiring a rather common technology.[9] However, the method requires ionic contrast between the internal and external GUVs solutions which the membranes might not be able to maintain as for instance in the case of transient pore formation, a phenomenon already observed during lipid oxidation.[6]

In the quest for a method to determine membrane area increase that is i) fast and easy, ii) effectively reliable even in the case of increased membrane permeability (due to transient pore formation or any other mechanism), we developed a bio-mimetic approach based on the geometrical changes that follow oxidation of GUVs strongly adhered on a substrate. The method can be easily implemented by simply i) preparing GUVs from a mixture of the desired lipids with a small fraction (2% or less) of commercially available biotinylated lipids, ii) let the giant vesicles sediment onto streptavidinated substrates also commercially available or prepared by well documented methods,[10-11] iii) measure the size of the vesicle adhesion patch by reflection interference contrast microscopy (RICM),[12] a technique available for standard optical microscopes, that can furthermore be implemented in a lighter version than the one commonly described in the literature, as explained into the SI section. As demonstrated below, one advantage of the technique stems from the easy and straightforward monitoring that no loss of internal liquid occurs during the experiment. Indeed, any membrane pore formation leads in the present geometry to a dramatic, easily detected decrease of the GUV volume, due to the strong adhesion conditions.

In this communication we show the feasibility and advantages of the method by measuring the area increase of POPC and DOPC GUVs oxidized in a solution of the photosensitizer erythrosin. Under irradiation at 547 nm, excited states of erythrosin can transfer energy to O_2, the molecular oxygen of the solution, thus generating singlet oxygen $^1O_2$.[13] This reactive oxygen species diffuses in the solution over an average length of 100 nm before decaying. Reactions of singlet oxygen with the unsaturated bonds of the lipid chains generate hydroperoxide groups that further induce an increase of area per lipid, due to the molecular-scale modification of the carbon chain hydrophilic-hydrophobic balance. In the present study we measure a specific area increase per lipid of circa 14% for POPC and 18% for DOPC, i.e. values that are in complete agreement with the

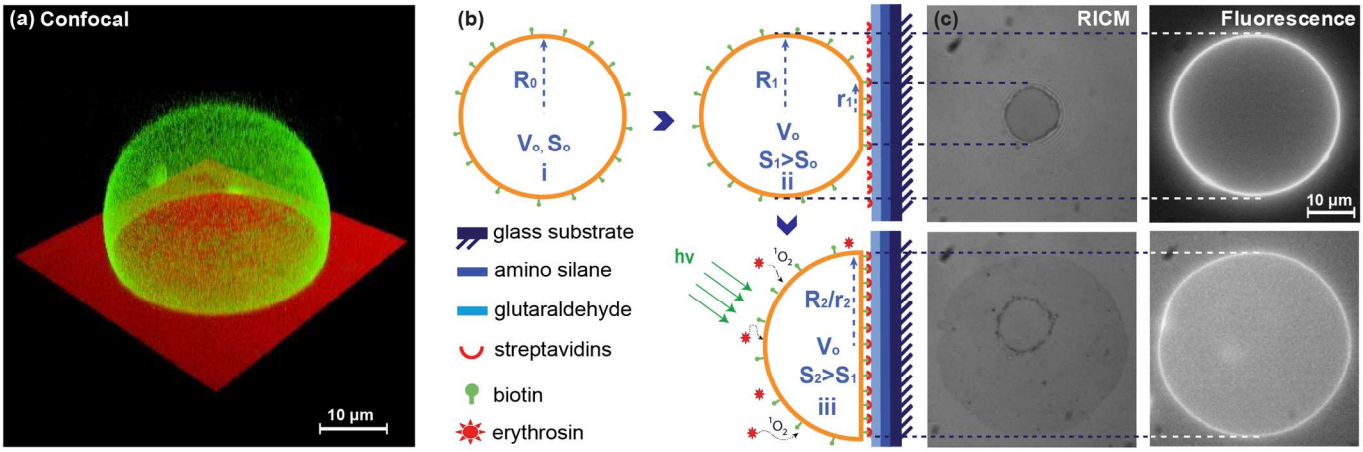

Fig.1 (a) Three-dimensional reconstitution of a typical adhered GUV, obtained from confocal microscopy. (b) Schematic representation of streptavidin molecularly-designed surfaces, biotinylated GUVs and the three-step sequence of the bio-adhesion method; i: free standing GUV as introduced in the observation cell; ii: non oxidized adhered GUV as obtained after sedimentation of the free standing GUVs; iii: oxidized GUV. GUVs and bio-molecule sizes do not fit true scale. (c) Biotinylated DOPC GUV adhered onto a streptavidin-covered surface, in a buffer containing 25 µM of erythrosin, as recorded with fluorescence microscopy and RICM, before (above) and after (below) irradiation.

Soft Matter RSCPublishing

COMMUNICATION

ones previously obtained by us on the same systems, using the micropipette aspiration technique.[8]

Our method relies on a two-step procedure. First, we prepare a substrate with adhered vesicles in the absence of any oxidation. Then, we oxidize the adhered vesicles and measure the associated membrane area increase. Figure 1a shows a three-dimensional reconstitution of a typical adhered GUV, obtained from confocal microscopy: the adhered vesicle has a shape composed of a circular adhered patch and a spherical section of radii r and R respectively (see the SI section for the justification of the GUV shape as a result of strong adhesion). The original GUVs, prepared in the bulk with radius R_0, volume V_0 and surface S_0 are driven down to the bottom of the observation cell, due to gravity forces, where they adhere in less than 10 seconds due to their strong affinity for the substrate surface, into a final shape with radii r_1 and R_1– see schemes I and II in Figure 1b. Figure 1c shows also how r_1 and R_1 can be determined by RICM and fluorescence microscopy respectively. As explained in SI, adhesion at that stage takes place at constant volume V_0 due to the sugar content of the solution; also, no vesicle bursting occurs under our strong adhesion conditions. This results in the increase of the apparent area of the vesicle from S_0 to S_1 corresponding to the unfolding of the original excess membrane, systematically present in GUVs obtained from electroformation, usually detected (in absence of any adhesion) by the presence of the thermally activated membrane fluctuations. Concomitantly to the membrane adhesion, the membrane tension increases up to a value where the Young's law for vesicle adhesion is obeyed.[14-16]At this point tension and adhesion forces are balanced.

For a transformation in vesicle shape at constant volume V_0, there is a one-to-one relation between the patch radius r and the membrane area S, as quantitatively explained in the supporting information and plotted in Figure 2a, where a theoretical projection of the relative surface area expansion (S/S_0-1) as a function of the reduced radius (r/R_0) of the adhered patch is shown. For typical experimental conditions this first step of adhesion results in a value for the radius r_1 of the adhesion patch of roughly 50%-70% of the original vesicle radius R_0. Due to the particular geometry of adhesion between the deformable spherical vesicle and the rigid flat substrate, such high adhesion patch sizes can be obtained by unfolding as little as 1% - 2% of excess membrane area, a feature clearly seen in the lower section of the curve in Figure 2a, as sketched by the region (ii). In our strong adhesion conditions, such unfolding corresponds to the complete smearing out of fluctuation modes without significantly stretching the membrane (see discussion in SI part). At this stage the prerequisite conditions for measuring photo-induced area increase are completed. However, for the purpose of checking the reliability of the technique, we verify systematically, i.e. for each studied GUV, the absence of internal volume loss during the oncoming oxidation step. We thus measure at that stage the adhesion patch radius r_1 and the equator radius R_1 of each adhered GUV to be oxidized (from RICM and fluorescence respectively), and calculate the GUV internal volume V_1 from equation 1 (see discussion in the SI section).

Then, as a second step we add erythrosin to the solution, so to reach a final concentration of 25 µM. This step does not perturb the adhered GUVs as evidenced by control experiments described in the SI section (see SI, Figure S1). Then constant illumination of the adhered vesicles in the oxidative solution starts, that leads to an increase of the membrane area due to the progressive hydroperoxidation of the lipids, as clearly illustrated by the supporting video and scheme III of Figure 1b. We monitor such increase by measuring under RICM the time evolution of the adhesion patch radius and converting it to the time variation of the relative excess area as plotted in Figure 2b. The surface area increases with time, eventually reaching a plateau. The kinetics of area increase is solely controlled by the production of oxidized lipid species. Indeed, not only immediate arrest follows if the irradiation is stopped (see SI, Figure S2), but also, as the inset in Figure 2b shows, is the rate of area production directly proportional to irradiation power.

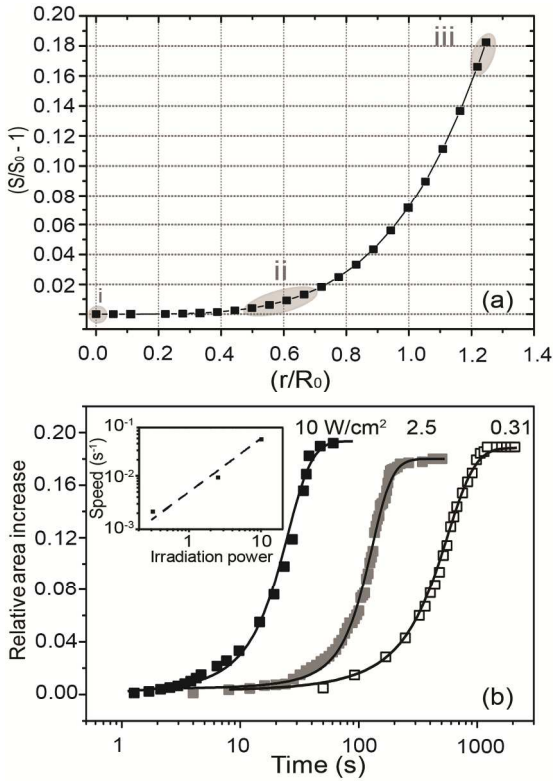

Fig. 2 (a) Theoretical projection of the relative surface area expansion (S/S_0-1) as a function of the reduced radius of the adhered patch (r/R_0), calculated from equations available at SI. (b) Evolution with time of relative surface area increase (S_2/S_1-1), considering different irradiation powers (10, 2.5 and 0.31 W/cm^2), for three DOPC GUVs. The inset shows the linear relation between the rate of area increase against time (speed s^{-1}) and irradiation power. The speed is determined by the slope of the linear regions of the curves.

Once the adhesion patch reaches its stable, maximum value, corresponding to full oxidation, irradiation is stopped and we measure again both adhesion patch radius r_2 and equator radius R_2in order to calculate the GUV volume V_2. Only if we measure V_2=V_1 within experimental error, the measured increase of membrane area

is considered as a reliable result. In fact, above 95% of the evaluated GUVs evolved without any leakage or bursting during oxidation. A full description of this results is given in the SI section (Figure S3) complemented by the discussion of the adhesion patch contrast loss (Figures S4 and S5). The remaining 5% proved that leakage and bursting correspond to events that are right away detectable, since they both deliver results far out of the mean statistics. Thus, the present method appears not only easy to implement but also trustable, a result mainly due to the strong adhesion conditions that create efficiently selective conditions for measuring membrane area increase.

Figure 3 shows histograms for the plateau values of the relative excess area curves; we find 14.3% and 18.4% for POPC and DOPC, respectively. These values are in very good agreement with results from the micropipette suction method recently published (i.e. 15.6% and 19.1% for POPC and DOPC).[8] It is also in good agreement with both recent Single Chain Mean Field theory predictions,[8] and consistent also with molecular simulations from Wong-Ekkabut et al.[17]

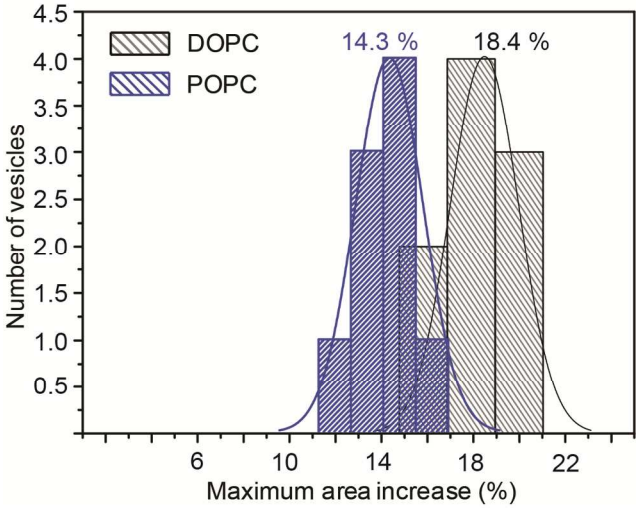

Fig. 3 Histograms built from the maximum relative surface area increase for DOPC and POPC (statistics obtained with 9vesicles for each lipid type).

Further comparison of our bio-adhesion method with in situ oxidation of GUVs under micropipette suction reveals very similar features. There,[8] not only the kinetic curves also reach a plateau, that corresponds to full oxidation of the lipid membrane, but one equally observes a direct relation between rate of area production and irradiation power as well as the immediate arrest of area production when irradiation is stopped. However, this standard technique requires a rather complex micromanipulation environment and a non-straightforward training for acquiring the appropriated manipulation skills. Besides, the photosensitizer aggregation into the micropipette is an issue that may hamper the measure of fully oxidized membrane. Although the drawback of the bio-adhesion method might be the use of biotinylated lipids, one can cite the fluorescent label-free and the RICM real time monitoring as advantages. Indeed, RICM is the only way to simultaneously irradiate the sample and follow the membrane transformations by using the same illumination source.

In summary, GUV adhesion on a bio-adhesive substrate provides a simple and powerful method for extracting molecular area increase of hydroperoxidized lipids. The major features of the method are its simplicity, quantitative nature and capacity to deal with any lipid species that can be self-assembled into a GUV. The method has also potential to quantitatively determine other oxidative processes that eventually lead to vesicle destruction, and can be straightforwardly extended to test the oxidation protection provided by antioxidant species. Although the method is here demonstrated for the particular case of lipid oxidation, it can be applied in many other situations where the area expansion of lipid membranes needs to be monitored, such as osmotic stresses, protein insertion or other oxidation mechanisms. In particular, since the method implies strong adhesion conditions to the membrane, it is particularly useful for processes that do not imply any particular increase of the membrane permeability as could happen from transient pore formation. By contrast, the method will clearly detect any permeation increase, which could be missed by gentler, external force-applying method, as for the electric field method.

Acknowledgements

This work was supported by Centre National de la Recherche Scientifique (CNRS) and is also part of a bilateral agreement USP-Cofecub (no Uc/Ph 124/11). Pedro H. B. Aoki acknowledges funding from Fundação de Amparo à Pesquisa do Estado de São Paulo (FAPESP 2012/01610-4).

Notes and references

[a] *Institut Charles Sadron, Universitéde Strasbourg, CNRS UP 22, F-67034 Strasbourg Cedex 2, France.*
[b] *Faculdade de Ciências e Tecnologia, UNESP Universidade Estadual Paulista, Presidente Prudente, SP, 19060-900, Brazil.*
[c] *São Carlos Institute of Physics, University of São Paulo, CP 369, 13560-970 São Carlos, SP, Brazil.*
Electronic Supplementary Information (ESI) available: [Experimental details]. See DOI: 10.1039/c000000x/

1 Citations here in the format A. Name, B. Name and C. Name, *Journal Title*, 2000, **35**, 3523; A. Name, B. Name and C. Name, *Journal Title*, 2000, **35**, 3523.

1. B. N. Ames, M. K. Shigenaga and T. M. Hagen, *Proceedings of the National Academy of Sciences of the United States of America*, 1993, **90**, 7915-7922.
2. E. L. Crockett, *Journal of Comparative Physiology B-Biochemical Systemic and Environmental Physiology*, 2008, **178**, 795-809.
3. W. Caetano, P. S. Haddad, R. Itri, D. Severino, V. C. Vieira, M. S. Baptista, A. P. Schroder and C. M. Marques, *Langmuir*, 2007, **23**, 1307-1314.
4. H. Sies, *Angewandte Chemie-International Edition in English*, 1986, **25**, 1058-1071.
5. S. P. Stratton and D. C. Liebler, *Biochemistry*, 1997, **36**, 12911-12920.
6. O. Mertins, Isabel O. L. Bacellar, F. Thalmann, Carlos M. Marques, Maurício S. Baptista and R. Itri, *Biophysical Journal*, 2014, **106**, 162-171.
7. K. A. Riske, T. P. Sudbrack, N. L. Archilha, A. F. Uchoa, A. P. Schroder, C. M. Marques, M. S. Baptista and R. Itri, *Biophysical Journal*, 2009, **97**, 1362-1370.

8. G. Weber, T. Charitat, M. S. Baptista, A. F. Uchoa, C. Pavani, H. C. Junqueira, Y. Guo, V. A. Baulin, R. Itri, C. M. Marques and A. P. Schroder, *Soft Matter*, 2014, **10**, 4241-4247.
9. R. Dimova, K. A. Riske, S. Aranda, N. Bezlyepkina, R. L. Knorr and R. Lipowsky, *Soft Matter*, 2007, **3**, 817-827.
10. R. Lehner, J. Koota, G. Maret and T. Gisler, *Physical Review Letters*, 2006, **96**.
11. M. L. Hisette, P. Haddad, T. Gisler, C. M. Marques and A. P. Schroder, *Soft Matter*, 2008, **4**, 828-832.
12. J. Radler and E. Sackmann, *Journal De Physique Ii*, 1993, **3**, 727-748.
13. D. S. Pellosi, B. M. Estevao, J. Semensato, D. Severino, M. S. Baptista, M. J. Politi, N. Hioka and W. Caetano, *Journal of Photochemistry and Photobiology a-Chemistry*, 2012, **247**, 8-15.
14. A. Albersdorfer, T. Feder and E. Sackmann, *Biophysical Journal*, 1997, **73**, 245-257.
15. R. Bruinsma and E. Sackmann, *Comptes Rendus De L Academie Des Sciences Serie Iv Physique Astrophysique*, 2001, **2**, 803-815.
16. D. Cuvelier and P. Nassoy, *Physical Review Letters*, 2004, **93**.
17. J. Wong-Ekkabut, Z. Xu, W. Triampo, I. M. Tang, D. P. Tieleman and L. Monticelli, *Biophysical Journal*, 2007, **93**, 4225-4236.

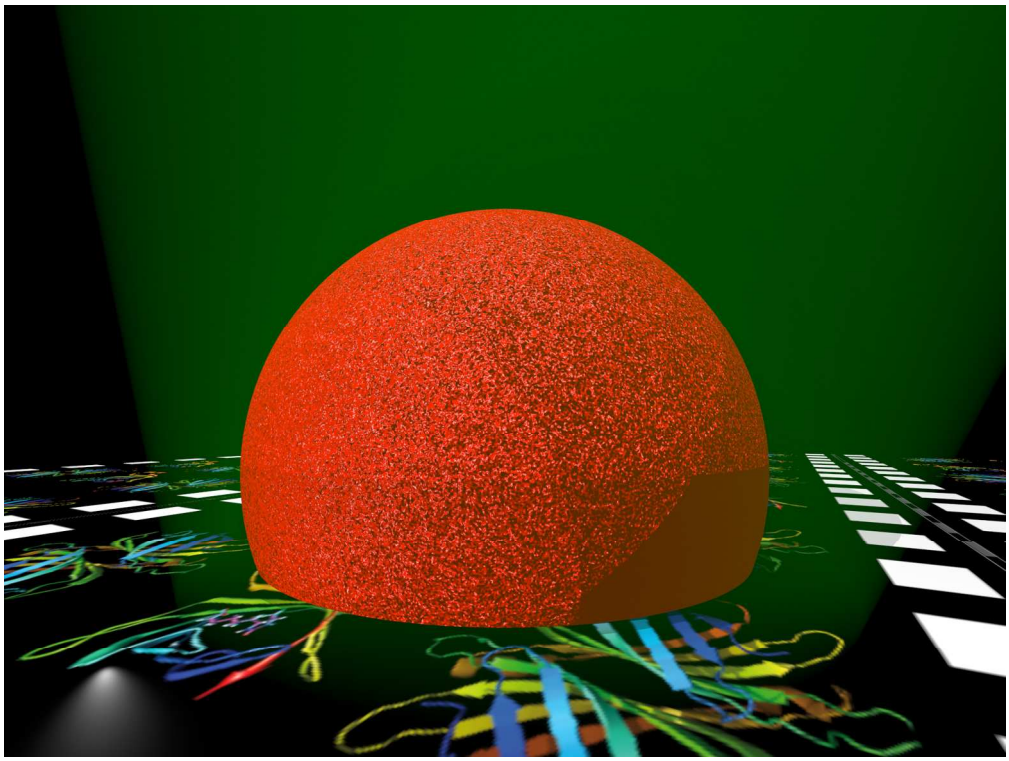

705x529mm (72 x 72 DPI)